Front. Med. 2023, 17(4): 685−698
https://doi.org/10.1007/s11684-022-0942-1

RESEARCH ARTICLE

ACSL5, a prognostic factor in acute myeloid leukemia, modulates the activity of Wnt/β-catenin signaling by palmitoylation modification

Wenle Ye[1,2,*], Jinghan Wang[1,2,*], Jiansong Huang[1,2], Xiao He[3], Zhixin Ma[4], Xia Li[1,2], Xin Huang[1,2], Fenglin Li[1,2], Shujuan Huang[1,2], Jiajia Pan[1,2], Jingrui Jin[1,2], Qing Ling[1,2], Yungui Wang[1,2], Yongping Yu[5], Jie Sun (✉)[1,2], Jie Jin (✉)[1,2,6]

[1]Department of Hematology, The First Affiliated Hospital, Zhejiang University College of Medicine, Hangzhou 310003, China; [2]Key Laboratory of Hematopoietic Malignancies, Diagnosis and Treatment, Hangzhou 310009, China; [3]Research Centre, Centre hospitalier de l'Université de Montréal (CRCHUM), Montreal, Quebec H2L 4M1, Canada; [4]Women's Hospital, School of Medicine, Zhejiang University, Hangzhou 310006, China; [5]Zhejiang Province Key Laboratory of Anti-Cancer Drug Research, College of Pharmaceutical Sciences, Zhejiang University, Hangzhou 310058, China; [6]Cancer Center, Zhejiang University, Hangzhou 310058, China

© Higher Education Press 2022

Abstract **Acyl-CoA synthetase long chain family member 5 (ACSL5), is a member of the acyl-CoA synthetases (ACSs) family that activates long chain fatty acids by catalyzing the synthesis of fatty acyl-CoAs. The dysregulation of ACSL5 has been reported in some cancers, such as glioma and colon cancers. However, little is known about the role of ACSL5 in acute myeloid leukemia (AML). We found that the expression of ACSL5 was higher in bone marrow cells from AML patients compared with that from healthy donors. ACSL5 level could serve as an independent prognostic predictor of the overall survival of AML patients. In AML cells, the ACSL5 knockdown inhibited cell growth both *in vitro* and *in vivo*. Mechanistically, the knockdown of ACSL5 suppressed the activation of the Wnt/β-catenin pathway by suppressing the palmitoylation modification of Wnt3a. Additionally, triacsin c, a pan-ACS family inhibitor, inhibited cell growth and robustly induced cell apoptosis when combined with ABT-199, the FDA approved BCL-2 inhibitor for AML therapy. Our results indicate that ACSL5 is a potential prognosis marker for AML and a promising pharmacological target for the treatment of molecularly stratified AML.**

Keywords acute myeloid leukemia; acyl-CoA synthetase long chain family member 5; Wnt3a; palmitoylation; ABT-199

Introduction

Acute myeloid leukemia (AML) is a clonal malignant disease characterized by an uncontrolled proliferation of undifferentiated myeloid precursors, resulting in impaired normal hematopoiesis [1]. Despite the emergence of novel treatment options approved for clinical practice in the past decades, the overall survival and relapse rates of AML patients have not been improved [2]. Therefore, a novel and personalized therapy for AML patients needs to be developed.

The acyl-CoA synthetase long chain family member 5 (ACSL5), which belongs to the family of acyl-conenzyme A (CoA) synthetases (ACSs), is deeply involved in the regulation of fatty acid metabolism. ACS family members esterify free fatty acids to acyl-CoAs, which is a key activation step necessary for the utilization of fatty acids [3,4]. Comparing with other identified isoenzymes, ACSL5 activates specific substrates of long-chain fatty acids with a backbone of 12 to 22 carbons and prefers to catalyze palmitate, palmitoleate, oleate, and linoleate [5]. ACSL5-knockout mice reported a 60% decrease in their palmitoyl-CoA synthesis rate [6]. Apart from its role in energy metabolism, palmitoyl-CoA also serves as a palmitate donor for palmitoylation modification, which is a specific post-transcriptional modification of proteins. ACSL5 is also involved in regulating Wnt2b protein palmitoylation modification [7]. Therefore, palmitoylated proteins can be regulated post-translationally by the

Received August 23, 2021; accepted June 6, 2022

Correspondence: Jie Jin, jiej0503@zju.edu.cn;
Jie Sun, sunjiehm@zju.edu.cn

*Wenle Ye and Jinghan Wang contributed equally to this work.

activity of ACSL5 via the palmitoyl-CoA level. Several studies have reported that ACSL5 functions as a tumor promoter in malignant glioma [8,9] and a tumor suppressor in colorectal carcinomas [10]. However, the biological and clinical significance of ACSL5 in AML has not yet been explored.

The Wnt family is involved in multiple developmental events during embryogenesis and has also been implicated in malignant disorders [11]. The functions of Wnt proteins are regulated by different post-translational modifications, including esterification and glycosylation [12,13]. Glycosylation plays a critical role in protein folding and stability [14], while esterification, specifically palmitoylation, is essential to Wnt secretion [15]. The depalmitoylation of serine 209 of Wnt 3a protein could induce Wnt3a retention in the endoplasmic reticulum and failure in secretion [16,17].

Triacsin c, a pan-ACS inhibitor, could inhibit the enzyme activity of ACS family members, including ACSL5, by competing with fatty acids for their catalytic domain [18]. This inhibitor has been reported to induce cytochrome c release and subsequent cell death via a functional apoptosome-mediated pathway, which can trigger antitumor activity in lung, colon, and brain cancer cells [19]. However, the antitumor effect of triacsin c in AML has not yet been explored.

In this study, we investigated the prognostic significance of ACSL5 in cytogenetically normal AML (CN-AML) patients and further demonstrated ACSL5 as an oncogenic protein that enhanced cell growth and inhibited cell apoptosis. ACSL5 deficiency drastically suppressed the Wnt/β-catenin signaling pathway via the inhibition of Wnt3a palmitoylation. Moreover, triacsin c exhibited an antileukemia effect in both AML cell lines and primary cells and worked synergistically with ABT-199, the selective BCL-2 inhibitor. Therefore, we propose that ACSL5 could serve as a novel biomarker in prognosis prediction and a tantalizing therapeutic target of AML.

Materials and methods

Patients

Bone marrow specimens were collected from healthy donors and 312 CN-AML patients at the First Affiliated Hospital, Zhejiang University School of Medicine from July 2010 to April 2016. The clinical samples of the participants were obtained directly after their diagnosis and before initiating treatment. Routine laboratory and clinical parameters were recorded. The gene mutation profiles of the patients, including *FLT3-ITD*, *NPM1*, *CEBPA*, *DNMT3A*, and *IDH1/2*, were detected through PCR and sequencing. This study was approved by the ethics committee of the hospital. Written informed consents were obtained from all participants, and the *Declaration of Helsinki* was followed.

Cell lines and primary cells

The AML cell lines THP-1, KG-1, and OCI-AML2 were purchased from Institute of Biochemistry and Cell Biology, Chinese Academy of Sciences, Shanghai, and THP-1-luciferase cell lines were donated by Professor Guido Marcucci of the City of Hope Medical Center and Beckman Research Institute, Duarte, California, USA. These cell lines were authenticated via DNA short-tandem repeat analysis by Shanghai Biowing Applied Biotechnology (Shanghai, China). THP-1, OCI-AML2, and KG-1 were routinely cultured in a Roswell Park Memorial Institute 1640 medium (RPMI-1640) supplemented with 10% fetal bovine serum (FBS) (Gibco). Primary AML cells were isolated via Ficoll-Hypaque (TBD Science, Tianjin, China) density gradient separation from the bone marrow samples of consenting patients who were newly diagnosed with AML. The primary cells were then cultured in a Stemspan serum-free medium II (SFEM II, StemCell Technologies) supplemented with recombinant human stem cell factor (IL-3, 25 ng/mL; IL-6, 10 ng/mL; Flt3L, 100 ng/mL; SCF, 50 ng/mL; TPO, 100 ng/mL). All cytokines were obtained from Pepro Tech US (Rocky Hill, NJ, USA). All cells were cultured at 37 °C with 5% CO_2 and high humidity.

RNA extraction and quantitative real-time PCR

Total RNA was extracted with the RNAiso Plus reagent (Takara, Japan) followed by cDNA synthesis with PrimerScript RT Master Mix (Takara, Japan). A quantitative real-time PCR analysis for determining the mRNA level was performed by using the one-step SYBR PrimeScript™ RT-qPCR Kit (Takara, Japan) operated on a IQ5 real-time PCR instrument (Bio-Rad, Hercules, CA). Relative RNA amount was calculated using the $2^{\Delta\Delta Ct}$ method normalized to GAPDH. The primers were purchased from Sangon Biotech (Shanghai, China) and summarized as follows: GAPDH-Fwd: 5′-ATGGGGAAGGTGAAGGTCG-3′ and GAPDH-Rev 5′-CTCCACGACGTACTCAGCG-3′; ACSL5-Fwd: 5′-GGCATTGGTGCTGATAGG-3′; and ACSL5-Rev: 5′-TCTTCTCCCCTCTTTGCTT-3′.

Lentiviral preparation, viral infection, and stable cell lines generation

Lentiviral plasmids expressing shACSL5 (#1, #2) or shCtrl and ACSL5-overexpression (ACSL5-OE) or empty vector were purchased from Genecopoeia. Stably

transduced cells were established following the procedure described in [20]. To summarize, the indicated plasmids were introduced into HEK293T together with lentiviral packaging vectors psPAX2 and pMD2.G using Lipofectamine 2000 (Life Technologies, 12566014). Viruses were collected 48 h and 72 h after transfection, and the target cells (THP-1, OCI-AML2 and KG-1) were infected with the collected viruses in the presence of polybrene (Sigma, 107689). The infected cells were selected with puromycin (2 μg/mL; Thermo Fisher) 2 days after infection.

Cell growth and viability assay

Cell growth and viability assay were measured via the CellTiter 96 Aqueous One Solution cell proliferation assay (Promega). The infected cells (1×10^4 cells/mL) were seeded in 96-well plates and mixed with an MTS solution before being incubated for 4 h at 37 °C. Absorbance was detected at 490 nm daily for 7 consecutive days. AML cell lines (1×10^5 cells/mL) or primary cells were plated in 96-well plates and treated with the indicated concentrations of drugs. Drug synergy was analyzed using the Combenefit software (Loewe model) [21]. The data were presented as means ± SEM from at least three independent experiments.

EdU assay

5-ethynyl-20-deoxyuridine (EdU) with Alexa-Fluor 594 dye kit (Beyotime, Shanghai, China) was used to measure cell proliferation ability. Cells were seeded with a density of 1×10^6 cells/mL and then incubated with a 10 μmol/L EdU buffer for 2 h at 37 °C, fixed with 4% formaldehyde for 15 min, and permeabilized with 0.3% Triton X-100 for 15 min. The results were assessed via flow cytometry.

Cell apoptosis and cell cycle assays

Cell apoptosis and cell cycle were analyzed via flow cytometry. For the apoptosis analysis, the cells were collected and stained with Annexin V-APC (or Annexin V-FITC) and PI at room temperature for 15 min. For the cell cycle analysis, the cells were harvested, fixed with 70% ethanol overnight at −20 °C prior to propidium iodide (PI) staining, and then analyzed immediately with a flow cytometer (NovoCyte, ACEA Biosciences). The data were analyzed using the NovoExpress software (ACEA Biosciences). Cell debris and dead cells were gated out for cell cycle analysis.

Western blot analysis

The cells were lysed in a RIPA buffer (Thermo Scientific, Waltham, MA) containing a protease and phosphatase inhibitor (Thermo Scientific, USA). Protein concentration was determined using the Bicinchoninic Acid Protein Assay Kit (Thermo Scientific, USA). The protein samples were separated by SDS-PAGE and transferred to 0.45 μm PVDF membranes (Millipore, USA). The membranes were blocked with 5% non-fat milk in TBST for 1 h, incubated overnight at 4 °C with primary antibodies, washed, and then incubated with HRP-linked specific secondary antibodies. Proteins were visualized with the ChemiDoc MP Imaging System (Bio-rad, Hercules, CA) using an enhanced chemiluminescence detection kit (Fdbio, China). GAPDH and β-tubulin were selected as loading controls. All antibodies employed in this study are listed below.

Antibodies and reagents

The antibodies for GAPDH (#5174), β-tubulin (#2146), PARP (#9532), and Caspase3 (#9662) were purchased from CST (MA, USA). The Wnt3a (ab219412), streptavidin-HRP (ab7403), and anti-human CD45-PE (ab27287) antibodies were purchased from Abcam (MA, USA), the anti-ACSL5 (15708-1-AP) antibody was purchased from ProteinTech (Rosemont, USA), triacsin c (10007448) was obtained from Cayman Chemical (MI, USA), and ABT-199 (S8048) was purchased from SELLECK (Shanghai, China).

TCF/LEF1 reporter assay

β-catenin activity was determined as luciferase transcription dependent on the T cell factor/lymphoid enhancer factor (TCF/LEF). The TCF/LEF1-luciferase reporter lentivirus was purchased from Genomeditech (Shanghai, China). Cells were infected with the reporter lentivirus and selected by 2 μg/mL puromycin for 2 days. Afterward, the cells were separately transduced with control and anti-ACSL5 shRNA lentivirus. At 72 h post transfection, the infection efficiency was estimated by determining the proportion of GFP-positive cells. Firefly luciferase activities were then assayed using the Dual-Luciferase Reporter Assay Kit (Promega, USA) according to protocol set by the manufacturer.

Metabolic labeling and click chemistry reaction

The cells were incubated with DMSO or 50 μmol/L palmitic acid analog ω-alkynyl palmitic acid Alk-C16 for 12 h. Labeled proteins bearing the alkyne group were then coupled with the azide group of biotin-azide or Azide Alexa Fluor 555 in click chemistry reaction. A click reaction solution was prepared in the following order: 0.1 mmol/L Azide Alexa Fluor 555 or biotin-azide, 1 mmol/L TCEP, 100 μmol/L TBTA, and 1 mmol/L $CuSO_4$ in ddH_2O.

Total palmitoylated proteins detected by flow cytometry: Alk-C16-labeled cells were fixed with 4% paraformaldehyde for 15 min and permeabilized with 0.3% TritonX-100 for 10 min at room temperature. The cells were then treated with click reaction solution containing Azide Alexa Fluor 555 for 30 min in the dark at room temperature. The fluorescence intensity of palmitoylated proteins was analyzed using the flowJo software.

Total palmitoylated proteins by western blot: after incubation, the cells were lysed in a lysis buffer containing 50 mmol/L TEA-HCl, pH 7.4, 150 mmol/L NaCl, 1% TritonX-100, 0.1% SDS, 1 × HALT protease, and phosphatase inhibitor cocktail (#78442, Thermo Scientific, USA). Lysates were cleared by centrifugation (13 000× *g* for 15 min at 4 °C). Supernatants were collected, and protein concentrations were determined using the BCA assay. An aliquot of 200 μg of protein from each sample was adjusted to 50 μL using a lysis buffer and then incubated with a click reaction solution containing biotin-azide. Biotinylated proteins were precipitated using methanol/chloroform and washed with methanol prior to air drying. The protein pellets were dissolved in a 1× SDS sample loading buffer. The samples were then subjected to western blot and immunoblotted with streptavidin-HRP.

Palmitoylated Wnt3a detected by western blot: the labeled cells were lysed, and the extracts were divided into input and IP samples (at about 1:5 ratio). The IP samples were incubated with anti-Wnt3a antibody and protein A/G beads. The Wnt3a proteins in the immunocomplexes captured with beads were then reacted with biotin-azide, subjected to SDS-PAGE, and immunoblotted with streptavidin-HRP. The streptavidin-HRP was stripped for 10 min in a Restore PLUS Western Blot Stripping Buffer (Thermo Scientific, USA), washed, blocked, and then incubated with the anti-Wnt3a antibody (1:1000 dilution). The input samples were subjected to western blot and immunoblotted with an anti-Wnt3a and β-tubulin antibody.

Leukemia xenograft model

A total of 18 female NOD-*Prkdc*^{scid}*IL2*rg^{tm1}/Bcgen (B-NSG) (age, 6–8 weeks; weight, 18–22 g; Biocytogen, China) were randomly sorted into two groups. Negative control THP-1-luc cells or stable ACSL5-Knockdown (ACSL5-KD) THP-1-luc cells were transduced and purified by cell sorting with a GFP marker 3 days after infection. Afterward, an equal number (1×10^6) of sorted cells were injected into two groups of mice separately through their tail veins. For bioluminescence imaging, the mice were anaesthetized with 3% isoflurane and then administered 100 mg/kg D-luciferin (Promega, USA) by intraperitoneal injection. The tumor load was monitored by bioluminescence imaging at days 14, 21, 28, and 35 post-transplantation, and the survival of mice was also recorded. Three mice from each group were sacrificed at day 35 post-transplantation, and the others were fed continuously to measure their survival. Murine bone marrow cells were obtained from their femur and tibia bone marrow, and their spleen and liver were harvested and weighed. All experimental procedures were conducted in accordance with the institution guidelines for care and use.

Gene set enrichment analysis (GSEA)

RNA-seq data from the transcriptome profile in the AML dataset were downloaded from TCGA. GSEA was performed using GSEA 3.0 (BROAD Institute). Normalized gene expression profiles were ranked by a signal-to-noise metric, and the normalized enrichment scores (NES) were calculated with random gene set permutation 1000. Significance was considered at a nominal *P* value (Nom *P* value) of < 0.05 and a false discovery rate (FDR) of 0.25.

Statistical analysis

A base line data comparison was conducted based on Student's *t*-test, Chi-square test, or one-way analysis of variance (ANOVA) depending on the needs. The survival data for the patients and mice were analyzed through the Cox regression model using the R package survival version 3.2-11. The experiments were repeated at least three times. The comparisons were performed using Student's *t*-test or one-way ANOVA. The data were presented as mean ± SD or SEM. *$P < 0.05$, **$P < 0.01$, and ***$P < 0.001$ indicated significant differences.

Results

High ACSL5 expression is associated with poor outcomes among AML patients.

To reveal the potential prognostic value of the ACSL5 mRNA expression for AML patients, we performed an explorative analysis of ACSL5 expression by exploring TCGA and GTEx datasets (via the GEPIA platform [22]). The expression of ACSL5 increased in the AML samples compared with the healthy donors ($P < 0.05$, Fig. 1A). The Kaplan–Meier survival analysis of the AML cohort from TCGA revealed that a high ACSL5 expression is associated with a poor overall survival for AML patients (Fig. 1B). The detailed clinical characteristics and multivariate analysis results of the TCGA cohort are shown in supplementary Tables S1 and S2, respectively. In addition, the $CD34^+$ hematopoietic stem cells from 6 healthy donors and the bone marrow mononuclear cells

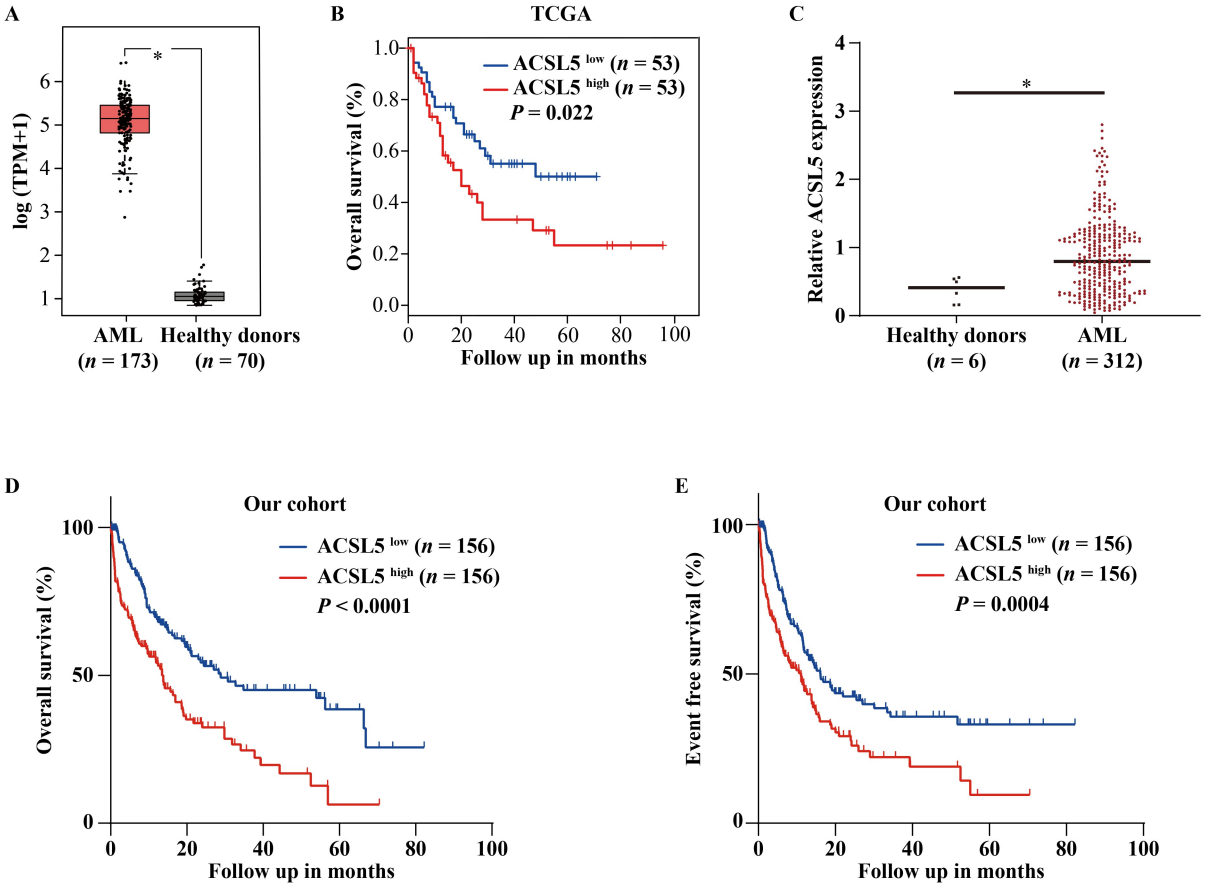

Fig. 1 High ACSL5 expression is associated with poor outcomes among AML patients. (A) The expression of ACSL5 mRNA in the TCGA and GTEx datasets was analyzed by GEPIA. **P* < 0.05, un-paired Student *t*-test. (B) Kaplan–Meier analysis of overall survival in the AML cohort from TCGA datasets. (C) RT-qPCR analysis showing ACSL5 expression in the bone marrow cells from AML patients (*n* = 312) and in the CD34 positive hematopoietic stem cells from healthy donors (*n* = 6). **P* = 0.032, un-paired Student *t*-test. (D,E) Kaplan–Meier analysis of overall survival (D) and event free survival (E) of 312 CN-AML patients. *P* value was calculated by log-rank tests.

from 312 CN-AML patients were collected. The mRNA levels of ACSL5 in AML patients were significantly higher than those in healthy individuals as confirmed by RT-qPCR (Fig. 1C). We further explored the correlation between the ACSL5 level in AML bone marrow cells and the outcomes of the 312 CN-AML patients. The AML patients with high ACSL5 expression (n = 156) had a relatively shorter overall survival (OS) ($P < 0.0001$) and event free survival (EFS) ($P = 0.0004$) compared with those in the low expression group (n = 156) (Fig. 1D and 1E). The baseline characteristics of the 312 CN-AML patients are provided in Table 1. A multivariate analysis of the OS and EFS of our cohort showed that the ACSL5 expression remained a poor prognostic factor (OS: HR = 1.932 (1.253, 2.979); EFS: HR = 1.544 (1.040, 2.293)) and an independent predictor (OS: $P = 0.003$; EFS: $P = 0.031$) after adjusting for age, WBC, gene mutation (including *FLT3-ITD* mutation, *NPM1, DNMT3A, CEBPA,* and *IDH1/2* mutations), and chemotherapy regimen (Table 2).

ACSL5 deficiency suppresses cell growth *in vitro*

To further investigate the role of ACSL5 in AML, we examined the mRNA and protein expressions of ACSL5 in a panel of AML cell lines (Fig. S1A and S1B). Among these cell lines, THP-1 and OCI-AML2 with a relatively high ACSL5 level and KG-1 with a relatively low ACSL5 expression were chosen for genetic manipulation to dissect the function of ACSL5. The efficiency of knockdown or overexpression of ACSL5 was determined by RT-qPCR and Western blot analysis. The MTS and EdU assays revealed that the reduction in ACSL5 expression was accompanied by an instantly diminished proliferative capabilities of THP-1 and OCI-AML2 cells (Fig. 2A–2D). By contrast, the overexpression of ACSL5 in KG-1 cells significantly promoted cell proliferation compared with those transduced with an empty vector (Fig. S1C–S1E). Furthermore, Annexin V/PI staining followed by flow cytometric analysis showed increased cell apoptosis in ACSL5 knockdown cells (Fig. 2E and

Table 1 Baseline characteristics of 312 CN-AML patients with low and high ACSL5 levels

Variables	Low expression	High expression	*P* value
Number (%)	156 (50.00)	156 (50.00)	
ACSL5 expression	0.42 (0.27, 0.64)	1.22 (1.09, 1.64)	< 0.0001
Age, median (range), year	51.00 (41.00, 61.00)	58.00 (37.00, 66.00)	0.1577
Male, *n* (%)	104 (66.67)	93 (59.62)	0.6812
[a]WBC, median ([b]IQR), $\times 10^9$/L	10.65 (2.30, 56.30)	13.10 (2.80, 54.00)	0.5373
[c]HB, median (IQR), $\times 10^9$/L	88.00 (69.00, 105.00)	84.00 (67.00, 102.00)	0.1241
[d]PLT, median (IQR), $\times 10^9$/L	52.00 (26.75, 90.75)	50.00 (27.75, 90.00)	0.9750
Blast, median (IQR), $\times 10^9$/L	65.00 (40.00,82.00)	69.00 (48.00,81.00)	0.2390
[e]FAB classification, *n* (%)			0.2934
M0	17 (10.90)	20 (12.82)	
M1	12 (7.69)	15 (9.62)	
M2	78 (50.00)	73 (46.79)	
M3	0	0	
M4	10 (6.41)	3 (1.92)	
M5	34 (21.79)	43 (27.56)	
M6	5 (3.21)	2 (1.28)	
Genes mutations, *n* (%)			
FLT3-ITD	26 (16.67)	35 (22.44)	0.6936
NPM1	41 (26.28)	42 (26.92)	0.3136
DNMT3A	16 (10.26)	20 (12.82)	0.6940
[f] $CEBPA^{DM}$	23 (14.74)	24 (15.38)	0.4400
IDH1	32 (20.51)	24 (15.38)	0.8987
IDH2	15 (9.62)	26 (16.67)	0.6859
[g]Treatment (%)			0.4445
DA	39 (25.00)	36 (23.08)	
HAA	34 (21.79)	17 (18.90)	
IA	83 (53.20)	103 (66.03)	
CR (%)	98 (62.82)	82 (52.56)	0.5097

[a]WBC, white blood cell; [b]IQR: interquartile; [c]HB, hemoglobin; [d]PLT: platelet counts; [e]FAB, French-American-British classification system; [f]DM, double-allele mutation; [g]The protocols used for induction therapy in different groups, including the daunorubicin/Ara-C (DA)-based treatment group, the idarubicin/Ara-C (IA)-based treatment group, and the homoharringtonine/Ara-C/aclarubicin (HAA)-based treatment group.

Table 2 Multiple analysis of OS and EFS in 312 CN-AML patients

Variables	Overall survival		Event free survival	
	HR (95% CI)	*P*	HR (95% CI)	*P*
ACSL5 expression (high vs. low)	1.932 (1.253, 2.979)	0.003	1.544 (1.040, 2.293)	0.031
Age (> 60)	2.191 (1.407, 3.413)	< 0.001	2.194 (1.455, 3.308)	< 0.001
WBC (> 10)	1.283 (0.836, 1.968)	0.254	1.487 (0.994, 2.224)	0.053
FLT3-ITD	2.332 (1.454, 3.740)	< 0.001	1.933 (1.240, 3.014)	0.004
NPM1	0.726 (0.447, 1.179)	0.196	0.838 (0.536, 1.309)	0.437
DNMT3a	1.839 (1.086, 3.115)	0.023	1.693 (1.030, 2.785)	0.038
CEBPA	0.286 (0.122, 0.670)	0.004	0.271 (0.123, 0.596)	0.001
IDH1	1.420 (0.827, 2.439)	0.204	1.631 (0.991, 2.685)	0.054
IDH2	1.160 (0.604, 2.226)	0.656	1.089 (0.594, 1.995)	0.078
Treatment protocols	1.098 (0.776, 1.553)	0.596	0.957 (0.688, 1.330)	0.792

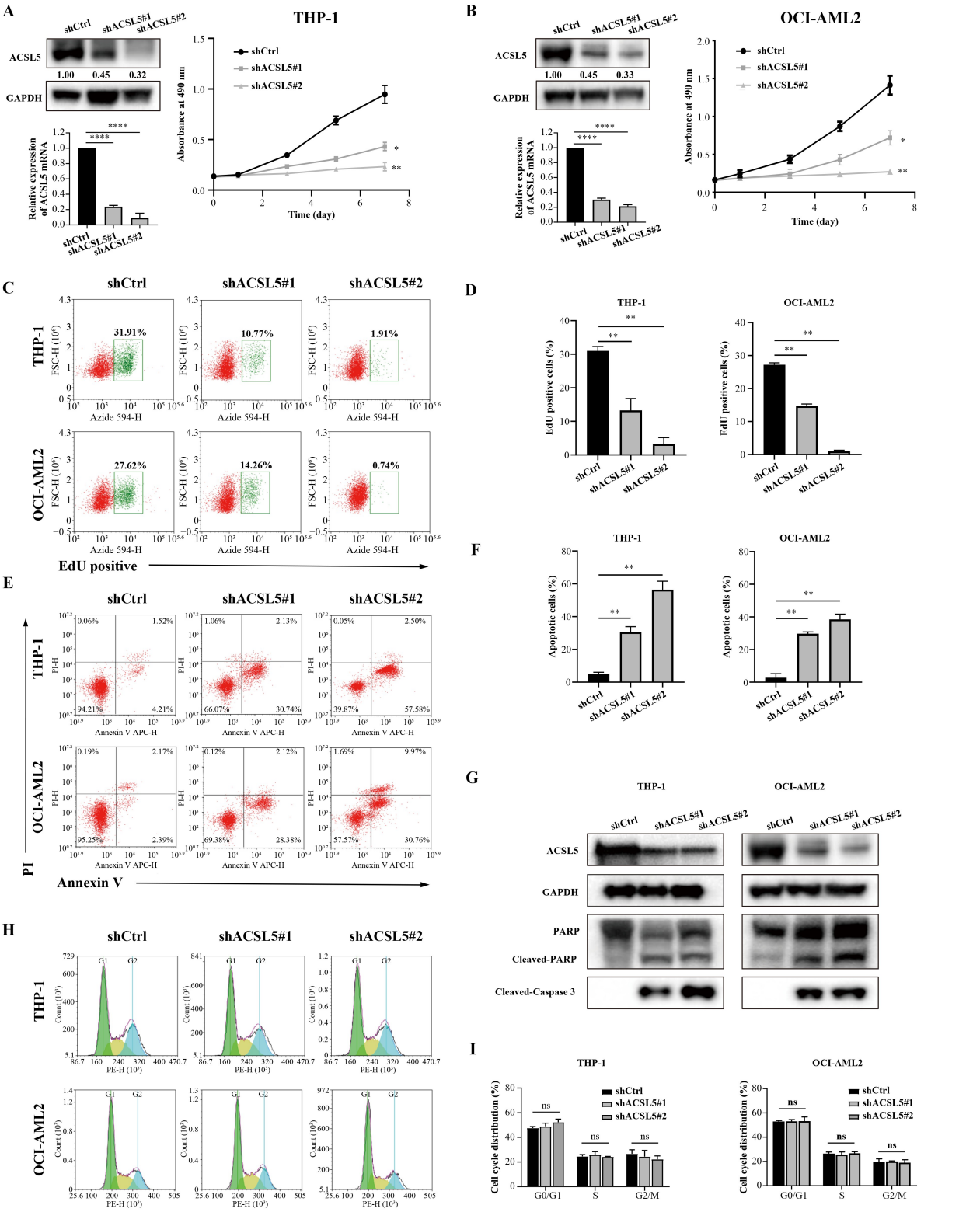

Fig. 2 ACSL5 deficiency suppresses cell growth *in vitro*. (A, B) Cell growth were detected by MTS in THP-1 (A) and OCI-AML2 (B) cells after transfected with negative control or shRNA (shACSL5#1 and #2). ACSL5 knockdown was confirmed by Western blot and qPCR. (C, D) EdU assay was utilized to detect cell proliferation ability after ACSL5 knockdown in THP-1 and OCI-AML2 cells; the EdU positive cells were determined by flow cytometry, and the summary data are presented in (D). (E, F) Annexin V/PI staining was measured by flow cytometry to determine apoptosis. Statistical results are shown in (F). (G) The cleavage of Caspase 3 and PARP was detected by Western blot in THP-1 and OCI-AML2 following the inhibition of ACSL5. (H, I) PI staining for cell cycle was analyzed. Representative result (H) and statistical bar charts (I) are shown.

2F). The ACSL5-deficiency-induced apoptosis in THP-1 and OCI-AML2 cells was also evidenced by cleaved Caspase 3 and PARP (Fig. 2G). The knockdown of ACSL5 had no apparent effects on cell cycle progression (Fig. 2H and 2I), and the ACSL5 overexpression did not produce an additional effect on cell apoptosis and cell cycle (Fig. S1F and S1G). Collectively, these results indicate that ACSL5 enhances AML cells expansion by promoting cell proliferation and inhibiting cell apoptosis.

Depletion of ACSL5 inhibits tumor growth in the AML xenograft model

To confirm the tumor-promoting role of ACSL5 *in vivo*, a xenograft mouse model was established by injecting THP-1-luc cells into B-NSG mice. The mice were randomly divided into two groups (nine mice per group) and were injected with control or ACSL5-knockdown THP-1-luc cells through their tail veins. Fluorescence imaging was performed at days 14, 21, 28, and 35 post-injection (Fig. 3A). The overall tumor burden of mice transplanted with ACSL5-knockdown cells was significantly lower than that observed in the control group (Fig. 3B). Moreover, the overall and median survival times of mice transplanted with ACSL5-KD cells were extended to 68 and 65 days, respectively, whereas that of the control group were merely 43 and 42 days (Fig. 3C). Three mice from each group were sacrificed at day 35 post-injection to evaluate the engraftment of human CD45 positive cells in BM cells and to weigh the livers and spleens. As expected, the proportion of human CD45 positive cells decreased in the BM of mice transplanted with ACSL5-KD cells compared with that in the BM of control mice (Fig. 3D). Likewise, the mice in the ACSL5-KD group indicated a significant reduction in their liver and spleen weights (Fig. 3E and 3F).

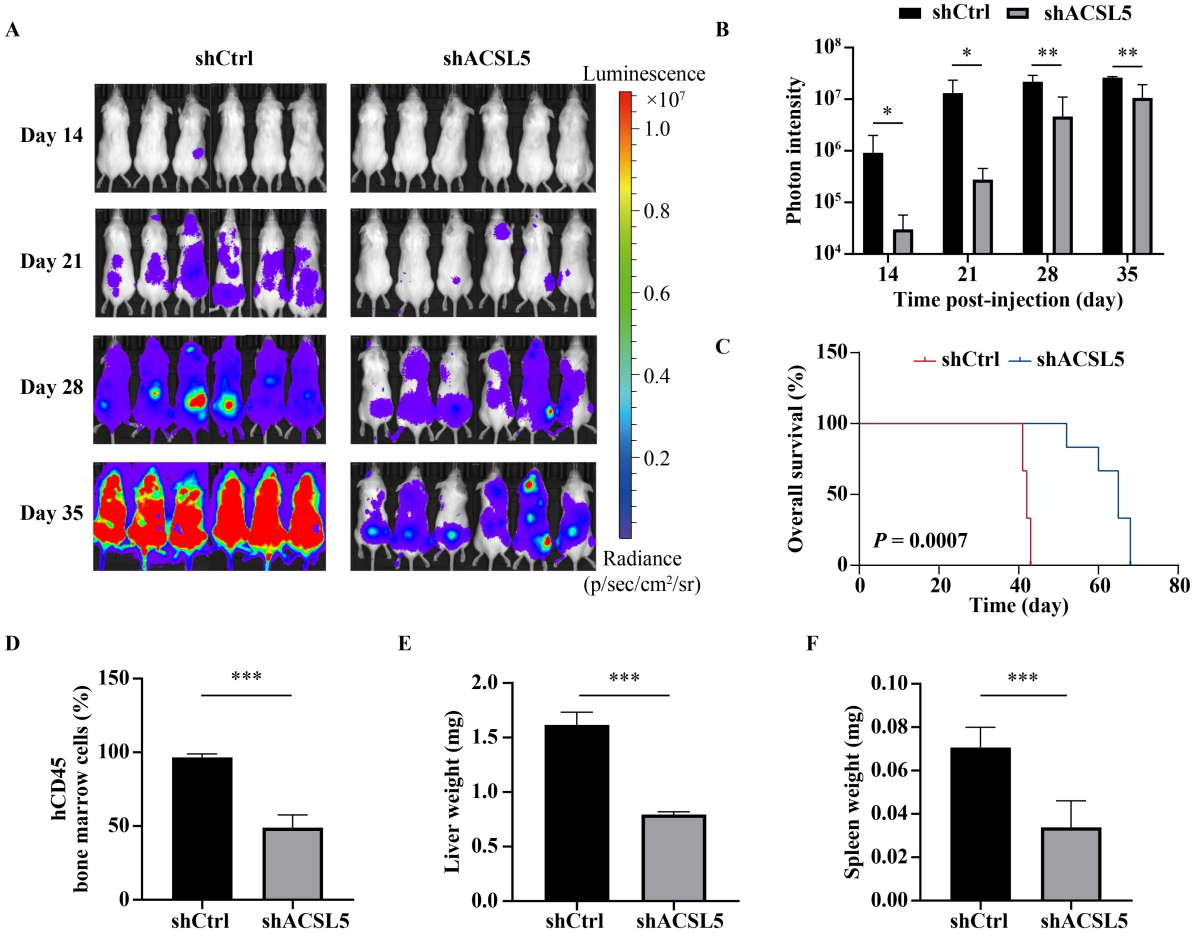

Fig. 3 Depletion of ACSL5 inhibits tumor growth in the leukemia xenograft model. (A) B-NSG mice were injected with THP-1-luc cells expressing shCtrl or shACSL5 through their tail veins. Live animal fluorescence imaging was carried out at days 14, 21, 28, and 35 post-injection. (B) Quantification of fluorescence images are expressed as mean ± SEM, $n = 6$ mice. (C) Kaplan–Meier survival curves of two groups of mice transplanted with shCtrl- or shACSL5-THP-1-luc cells ($n = 6$ mice per group). Statistical significance in survival was determined via log-rank test. ***$P < 0.001$ compared with the shCtrl group. (D–F) Three mice in the shCtrl or shACSL5 group were sacrificed at day 35 post-injection. The proportion of hCD45 positive blasts in the bone marrow of mice from different groups was determined by flow cytometry (D); Livers (E) and spleens (F) were harvested and weighted. The values are expressed as the mean ± SEM of 3 mice (***$P < 0.0001$, unpaired Student's *t*-test).

ACSL5 modulates the activity of Wnt/β-catenin signaling by palmitoylation modification

To determine through which pathway ACSL5 promotes AML cell growth, we performed GSEA analysis based on mRNA expression data of an AML cohort from the TCGA database. Results of the GSEA analysis strongly implicated Wnt/β-catenin signaling as the main biological process affected by ACSL5 (Fig. 4A). Knockdown of ACSL5 significantly reduced the Wnt signaling response, which was accompanied by an increase in GSK-3β phosphorylation and a reduction in β-catenin accumulation in THP-1 and OCI-AML2 cells (Fig. 4B). We further used the TCF/LEF reporter assay to investigate whether ACSL5 influenced the activity of the Wnt/β-catenin signaling pathway, and the results revealed that the inhibition of ACSL5 significantly downregulated TCF/LEF-dependent luciferase activity (Fig. 4C). Meanwhile, the click chemistry assay revealed that the knockdown of ACSL5 induced a significant decrease in the palmitoylation of whole proteins (Fig. 4D) and the Wnt3a protein (Fig. 4E).

Triacsin c, the pan-ACS inhibitor, exerts a synergistic inhibition effect with ABT-199 in AML cells

To investigate the therapeutic potential of triacsin c (a pan-ACS inhibitor) in AML, we analyzed the responses of human AML cells to triacsin c *in vitro*. Triacsin c inhibited cell growth in six AML cell lines in a concentration-dependent manner at 48 h. Among the tested cell lines, the IC_{50} values of THP-1 and OCI-AML2 were 0.4671 ± 0.0531 μmol/L and 0.3683 ± 0.0232 μmol/L respectively, whereas those of the other AML cells are shown in supplementary Fig. S2A. Those cells treated with increasing concentrations of triacsin c showed an increased rate of apoptosis (Fig. S2B and S2C). We hypothesized a potential synergistic effect between triacsin c and ABT-199, the BCL2-selective inhibitor, that could induce a more intense cell apoptosis. To this end, we treated THP-1 and OCI-AML2 cells with triacsin c or ABT-199 either alone or in combination. Consistent with our hypothesis, we observed synergistic effects at triacsin c concentrations of 0.25 μmol/L to 1 μmol/L when combined with ABT-199 in both THP-1 and OCI-AML2 cells (Figs. 5A and 5B). Moreover, the combined treatment significantly increased apoptosis as evidenced by the increase in Annexin V stained cells and cleaved Caspase 3 and PARP levels compared with cells treated with either triacsin c or ABT-199 (Figs. 5C, 5D and S5D). Moreover, triacsin c substantially inhibited cell growth in primary cells but did not exhibit cytotoxicity to normal $CD34^+$ cells (Fig. 5E and 5F). We further measured the sensitivity of triacsin c and the expression level of ACSL5 in AML primary cells (AML#6 to #15). However, we found no significant association between the ACSL5 level and IC_{50} of triacsin c in the Spearman rank correlation analysis (Fig. S4). In addition, the combination treatments of triacsin c or ABT-199 in primary cells (AML#16 to #18) were significantly more efficient than the single treatment (Fig. 5G–5I).

Discussion

ACSL5 has a special position among acyl-CoA synthetases given its distinct subcellular localization on the mitochondrial membrane and strong preference for palmitate and palmitoleic acids [4]. ACSL5 was identified as a functional regulator for cells to sustain their proliferation and resistance to cell death. Mashima *et al*. reported that ACSL5 could help improve glioma cell survival under extracellular acidosis conditions [8]. Moreover, long-chain acyl-CoA esters, as the products of ACSL5, are important intermediates in lipid biochemistry and have been reported to affect several aspects of cellular functions and signaling pathways [23]. We demonstrated that ACSL5 facilitated the growth of AML cell lines *in vitro* and *in vivo* based on the stable ACSL5 knockdown or overexpression cells.

We also observed that the inhibition of ACSL5 increased the GSK-3β phosphorylation and degraded β-catenin, which in turn inhibited the activity of the Wnt signaling pathway. ACSL5 plays a crucial role in the palmitate metabolic process as it converts palmitate into its active form, namely, palmitoyl-CoA [23]. Palmitoyl-CoA serves as a palmitate donor for Wnt3a palmitoylation. The knockout of Acsl5 showed a 60% reduction in jejunal palmitoyl-CoA synthesis rate and did not alter the mRNA expression of the other major isoforms of ACSL [6]. Collectively, LC-MS/MS demonstrated a positive correlation between ACSL5 activity and acyl-CoA synthesis, particularly for less abundant sphingolipid species and saturated acyl-CoA species, such as palmitate [24]. Therefore, we could reasonably assume that ACSL5 may play its function by directing the cellular metabolism of palmitate and regulating the palmitoylation level of key proteins.

Palmitoylation is a specific form of post-translational modification that involves the thioesterification of a 16-carbon saturated fatty acid (palmitate) [25]. This palmitoylation can regulate the localization, accumulation, secretion, stability, and function of proteins by altering their membrane affinity [26]. Indeed, the lipidation of some key signaling proteins, such as Hedgehog, Wnt, and RAS, is essential for their function both physiologically and in cancer [25,26]. The functional association of fatty acid metabolizing enzymes to the modification of Wnt proteins is of high importance in building a molecular link between cell intrinsic fatty acid metabolism and the

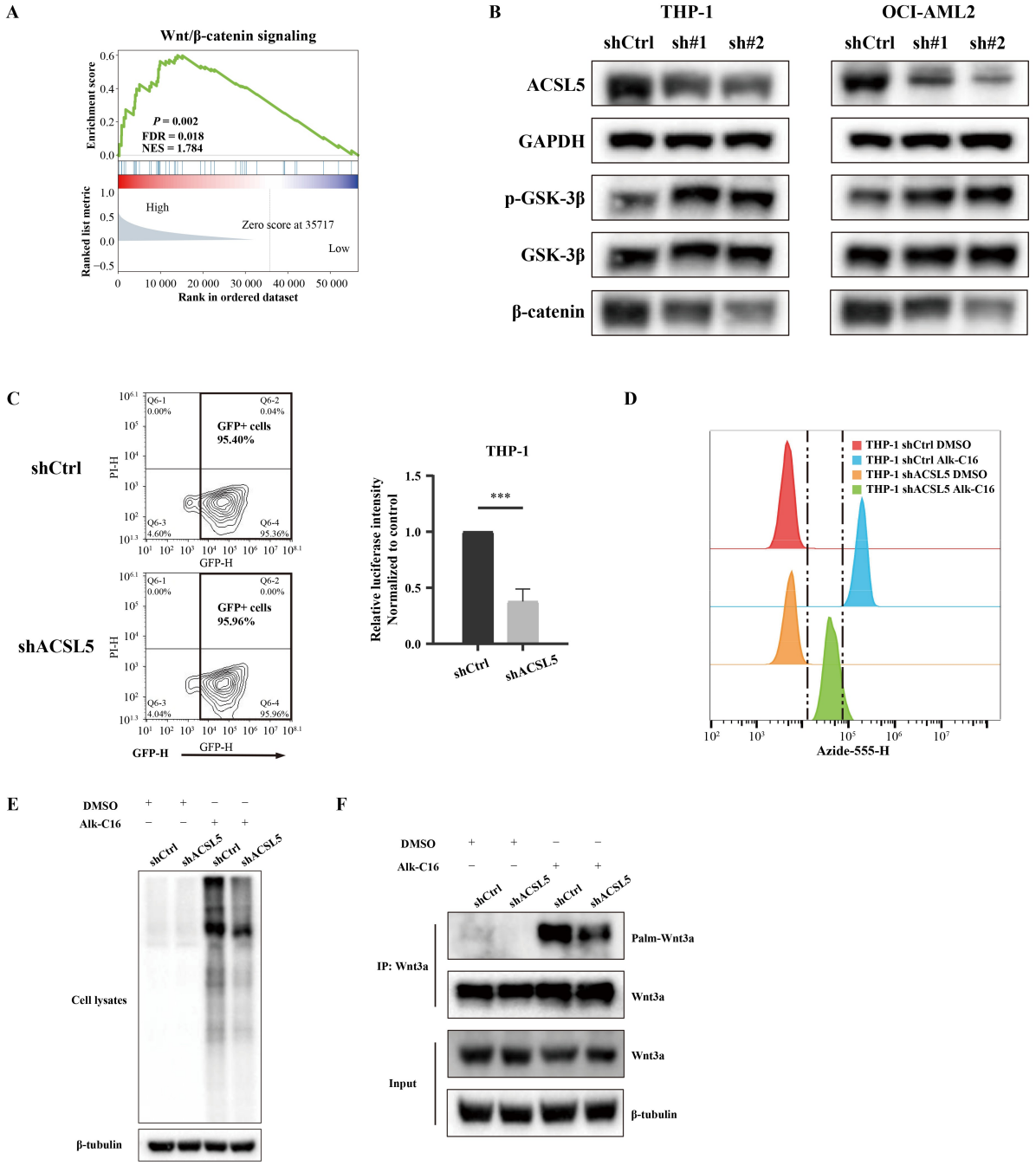

Fig. 4 Knockdown of ACSL5 downregulated the Wnt/β-catenin signaling pathway by reducing the palmitoylation modification of the Wnt3a protein. (A) The GSEA identified Wnt/β-catenin-signaling-related genes as being upregulated in AML patients with a high expression of ACSL5 (NES = 1.784, FDR = 0.018). (B) Western blot was performed for p-GSK-3β, total-GSK-3β, and total-β-catenin. (C) THP-1 was infected with TCF/LEF1-luciferase reporter lentivirus and selected by 2 μg/mL puromycin for 2 days. These cells were further infected with GFP-labeled lentivirus encoding ACSL5 shRNA and nontargeting shRNA. The transfection efficiency, as confirmed by GFP expression, was greater than 95% at 72 h post-infection by flow cytometry (left). One million live cells were harvested and subjected to TCF/LEF reporter assay to determine the activity of the Wnt/β-catenin signaling pathway (right, ***P = 0.0006, unpaired Student's t-test). (D, E) Control and ACSL5-knockdown THP-1 cells were incubated with DMSO or 50 μmol/L palmitic acid analog Alk-C16 for 12 h. The incorporated Alk-C16 of total protein was detected by flow cytometry (D) and Western blotting (E). (F) After incubation with Alk-C16, the THP-1 cells were lysed and immunoprecipitated with the anti-Wnt3a antibody. The immunoprecipitate was reacted with biotin-azide, and the palmitoylated Wnt3a was detected by Western blot.

critical signaling pathway. Our study demonstrated that the suppression of ACSL5 decreased the level of Wnt3a palmitoylation modification, which accounted for the inhibition of the Wnt/β-catenin signaling pathway.

Wnt signaling has been strongly associated with a variety of cancers [27,28]. The aberrant activation of Wnt

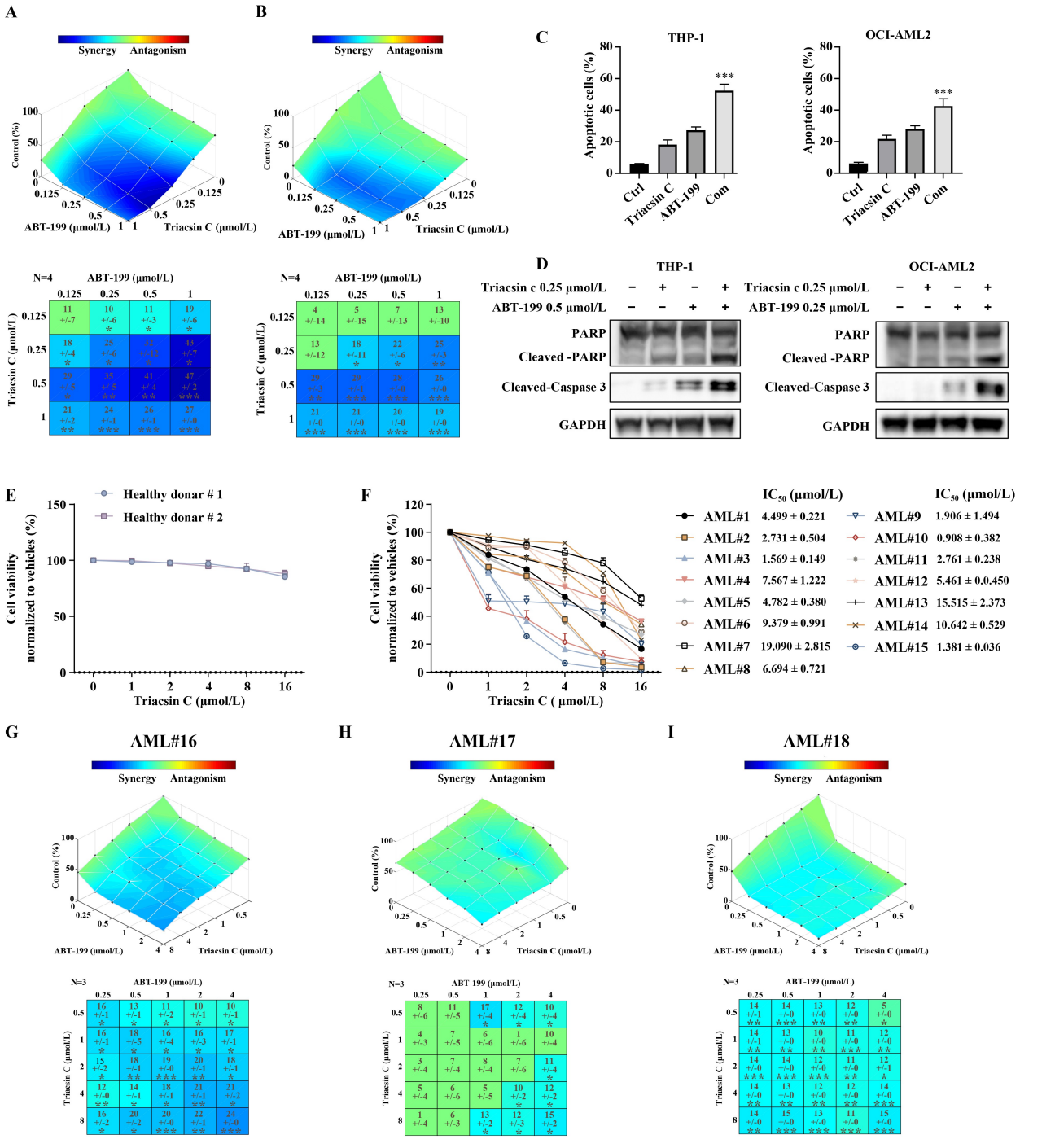

Fig. 5 Triacsin c, the ACS inhibitor, exerts a synergistic inhibition effect with ABT-199 in AML cells. (A, B) THP-1 and OCI-AML2 cells were treated for 48 h as indicated with triacsin c and ABT-199 and were analyzed for cell viability via MTS assay. The drug synergy/antagonism was calculated by using the Loewe Addictivity method via the Combenefit software. The synergy score of the drug combination was expressed as mean ± SD (n = 4 replicates). (C) Apoptosis was analyzed by flow cytometry in the THP-1 and OCI-AML2 cells following treatment as indicated with triacsin c and ABT-199 at 48 h. (D) The levels of cleaved caspase 3 and PARP were determined by Western blot assays. (E) Cell viability inhibited by triacsin c after 48 h in $CD34^+$ cells isolated from two independent cord blood samples. (F) Triacsin c inhibited cell growth in primary AML cells at 48 h. (G–I) Cell viability of primary AML cells was measured by MTS assay after triacsin c or ABT-199 monotherapy or their combination therapy at 48 h. The combination effect was analyzed using the Combenefit software. The data were presented as mean ± SD from at least three independent experiments.

signaling is a frequent yet heterogenous feature of AML [29]. Wnt/β-catenin pathway is required in the self-renewal of leukemia stem cells [30]. The canonical Wnt pathway is activated upon the binding of secreted Wnt

proteins to its receptor Frizzled (FZD) in complex with co-receptors LPR5/6 at the plasma membrane. Subsequently, the β-catenin is dephosphorylated and stabilized from the destruction complex. β-catenin accumulates and translocates into the nucleus where it interacts with the TCF/LEF transcription factor family to drive a downstream gene expression [29].

We found strong evidence to suggest that the palmitoylation in Wnt3a protein is involved in intracellular trafficking during the secretory process. Although Wnt3a was originally reported to be fatty acylated at Cysteine 77 [31], Gao and Nile *et al*. demonstrated that Cys 77 is unlikely to be available for fatty acylation [32,33]. Wnt3a was palmitoylated by O-acyl-transferase — porcupine at Serine 209 but not Cys77. The palmitoylation at Serine 209 of the Wnt3a protein was reported by metabolic labeling with a radiolabeled palmitate. The Wnt3a with acylation defect at Ser209 was not secreted from cells in culture and was instead retained in the endoplasmic reticulum. Ser209-dependent acylation may be required for targeting Wnt3a proteins to specific organelles or membrane components for secretion [32,34]. Therefore, we hypothesized that the altered palmitoylation of Wnt3a induced by ACSL5 knockdown was responsible for the defective Wnt/β-catenin response.

Accumulating evidence suggests that the dysregulation of ACSL5 is involved in various cancers, including glioma, colon cancer, and lung cancer [8,35–37]. Therefore, ACSL5 was considered a diagnostic and prognostic marker and a potential therapeutic target against cancer. However, its clinical significance has not been elucidated in AML. In this study, we revealed for the first time that the expression of ACSL5 was elevated in BM samples of AML patients. A high expression of ACSL5 was also associated with poor overall survival in AML.

Triacsin c is an inhibitor of ACS family that competes with fatty acids for their catalytic domain [38]. Triacsin c could induce massive apoptosis in glioma cells, whereas cell death was completely suppressed by the overexpression of ACSL5 [39]. Furthermore, in terms of p53-defective tumor cell lines, triacsin c could selectively induce apoptosome-mediated cell death in tumor cells [19,39]. In line with these findings, the treatment of triacsin c induced cell apoptosis in AML cell lines and primary cells. ABT-199, an FDA-approved BCL-2 selective inhibitor, could disrupt the interaction between Bim and BCL-2, thereby freeing the former to induce apoptosis [40]. Unlike most oncogenic proteins, BCL-2 dysregulation does not confer an advantage in cell growth or proliferation but instead allows cells that would normally undergo apoptosis to survive. Some cancer cells approach the threshold of apoptosis but are held back from death by BCL-2 family proteins that favor their survival [41]. In our study, we found that the inhibition of ACSL5, either by triacsin c or shRNA lentivirus, significantly promotes cell apoptosis, hence leading us to wonder whether the addition of ABT-199, which directly targets apoptosis, could push cells on the verge of breakdown toward apoptosis. Triacsin c exhibited a synergistic effect with ABT-199, thereby suggesting that triacsin C has the potential to be an effective anti-leukemia agent alone or combined with ABT-199. In conclusion, we demonstrated for the first time that ACSL5 is a reliable prognosis marker and a potential therapeutic target for AML.

Acknowledgements

We thank Prof. Guido Marcucci of the City of Hope Medical Center and Beckman Research Institute, Duarte, California, USA, for providing us the THP-1-luciferase cell line. This work was supported by the key international cooperation projects of the National Natural Science Foundation of China (No. 81820108004), the major projects of the Zhejiang Provincial Department of Science and Technology (No. 2021C03123), and the Pediatric Leukemia Diagnosis and Therapeutic Technology Research Center of Zhejiang Province (No. JBZX-201904).

Compliance with ethics guidelines

Wenle Ye, Jinghan Wang, Jiansong Huang, Xiao He, Zhixin Ma, Xia Li, Xin Huang, Fenglin Li, Shujuan Huang, Jiajia Pan, Jingrui Jin, Qing Ling, Yungui Wang, Yongping Yu, Jie Sun, and Jie Jin declare no conflict of interest. This study was approved by the ethics committee of the First Affiliated Hospital of Zhejiang University. All procedures followed were in accordance with the ethical standards of the responsible committees on human experimentation (institutional and national) and with the *Helsinki Declaration* of 1975 as revised in 2000. Informed consents were obtained from all patients participating in this study. All institutional and national guidelines for the care and use of laboratory animals were also followed.

Electronic Supplementary Material Supplementary material is available in the online version of this article at https://doi.org/10.1007/s11684-022-0942-1 and is accessible for authorized users.

References

1. Yan P, Frankhouser D, Murphy M, Tam HH, Rodriguez B, Curfman J, Trimarchi M, Geyer S, Wu YZ, Whitman SP, Metzeler K, Walker A, Klisovic R, Jacob S, Grever MR, Byrd JC, Bloomfield CD, Garzon R, Blum W, Caligiuri MA, Bundschuh R, Marcucci G. Genome-wide methylation profiling in decitabine-treated patients with acute myeloid leukemia. Blood 2012; 120(12): 2466–2474
2. Roboz GJ. Current treatment of acute myeloid leukemia. Curr Opin Oncol 2012; 24(6): 711–719

3. Watkins PA, Maiguel D, Jia Z, Pevsner J. Evidence for 26 distinct acyl-coenzyme A synthetase genes in the human genome. J Lipid Res 2007; 48(12): 2736–2750
4. Ellis JM, Frahm JL, Li LO, Coleman RA. Acyl-coenzyme A synthetases in metabolic control. Curr Opin Lipidol 2010; 21(3): 212–217
5. Klett EL, Chen S, Yechoor A, Lih FB, Coleman RA. Long-chain acyl-CoA synthetase isoforms differ in preferences for eicosanoid species and long-chain fatty acids. J Lipid Res 2017; 58(5): 884–894
6. Meller N, Morgan ME, Wong WP, Altemus JB, Sehayek E. Targeting of acyl-CoA synthetase 5 decreases jejunal fatty acid activation with no effect on dietary long-chain fatty acid absorption. Lipids Health Dis 2013; 12(1): 88
7. Klaus C, Schneider U, Hedberg C, Schütz AK, Bernhagen J, Waldmann H, Gassler N, Kaemmerer E. Modulating effects of acyl-CoA synthetase 5-derived mitochondrial Wnt2B palmitoylation on intestinal Wnt activity. World J Gastroenterol 2014; 20(40): 14855–14864
8. Mashima T, Sato S, Sugimoto Y, Tsuruo T, Seimiya H. Promotion of glioma cell survival by acyl-CoA synthetase 5 under extracellular acidosis conditions. Oncogene 2009; 28(1): 9–19
9. Mashima T, Sato S, Okabe S, Miyata S, Matsuura M, Sugimoto Y, Tsuruo T, Seimiya H. Acyl-CoA synthetase as a cancer survival factor: its inhibition enhances the efficacy of etoposide. Cancer Sci 2009; 100(8): 1556–1562
10. Hartmann F, Sparla D, Tute E, Tamm M, Schneider U, Jeon MK, Kasperk R, Gassler N, Kaemmerer E. Low acyl-CoA synthetase 5 expression in colorectal carcinomas is prognostic for early tumour recurrence. Pathol Res Pract 2017; 213(3): 261–266
11. Logan CY, Nusse R. The Wnt signaling pathway in development and disease. Annu Rev Cell Dev Biol 2004; 20(1): 781–810
12. Yang Y. Wnt signaling in development and disease. Cell Biosci 2012; 2(1): 14
13. Nusse R, Clevers H. Wnt/β-catenin signaling, disease, and emerging therapeutic modalities. Cell 2017; 169(6): 985–999
14. Roth J, Zuber C, Park S, Jang I, Lee Y, Kysela KG, Le Fourn V, Santimaria R, Guhl B, Cho JW. Protein N-glycosylation, protein folding, and protein quality control. Mol Cells 2010; 30(6): 497–506
15. Willert K, Nusse R. Wnt proteins. Cold Spring Harb Perspect Biol 2012; 4(9): a007864
16. Takada R, Satomi Y, Kurata T, Ueno N, Norioka S, Kondoh H, Takao T, Takada S. Monounsaturated fatty acid modification of Wnt protein: its role in Wnt secretion. Dev Cell 2006; 11(6): 791–801
17. Hausmann G, Bänziger C, Basler K. Helping Wingless take flight: how WNT proteins are secreted. Nat Rev Mol Cell Biol 2007; 8(4): 331–336
18. Kaemmerer E, Peuscher A, Reinartz A, Liedtke C, Weiskirchen R, Kopitz J, Gassler N. Human intestinal acyl-CoA synthetase 5 is sensitive to the inhibitor triacsin C. World J Gastroenterol 2011; 17(44): 4883–4889
19. Mashima T, Oh-hara T, Sato S, Mochizuki M, Sugimoto Y, Yamazaki K, Hamada J, Tada M, Moriuchi T, Ishikawa Y, Kato Y, Tomoda H, Yamori T, Tsuruo T. p53-defective tumors with a functional apoptosome-mediated pathway: a new therapeutic target. J Natl Cancer Inst 2005; 97(10): 765–777
20. Marino MP, Luce MJ, Reiser J. Small- to large-scale production of lentivirus vectors. Methods Mol Biol 2003; 229: 43–55
21. Di Veroli GY, Fornari C, Wang D, Mollard S, Bramhall JL, Richards FM, Jodrell DI. Combenefit: an interactive platform for the analysis and visualization of drug combinations. Bioinformatics 2016; 32(18): 2866–2868
22. Tang Z, Li C, Kang B, Gao G, Li C, Zhang Z. GEPIA: a web server for cancer and normal gene expression profiling and interactive analyses. Nucleic Acids Res 2017; 45(W1): W98–W102
23. Chopard C, Tong PBV, Tóth P, Schatz M, Yezid H, Debaisieux S, Mettling C, Gross A, Pugnière M, Tu A, Strub JM, Mesnard JM, Vitale N, Beaumelle B. Cyclophilin A enables specific HIV-1 Tat palmitoylation and accumulation in uninfected cells. Nat Commun 2018; 9(1): 2251
24. Klaus C, Kaemmerer E, Reinartz A, Schneider U, Plum P, Jeon MK, Hose J, Hartmann F, Schnölzer M, Wagner N, Kopitz J, Gassler N. TP53 status regulates ACSL5-induced expression of mitochondrial mortalin in enterocytes and colorectal adenocarcinomas. Cell Tissue Res 2014; 357(1): 267–278
25. Ko PJ, Dixon SJ. Protein palmitoylation and cancer. EMBO Rep 2018; 19(10): e46666
26. Fhu CW, Ali A. Protein lipidation by palmitoylation and myristoylation in cancer. Front Cell Dev Biol 2021; 9: 673647
27. MacDonald BT, Tamai K, He X. Wnt/beta-catenin signaling: components, mechanisms, and diseases. Dev Cell 2009; 17(1): 9–26
28. Zhan T, Rindtorff N, Boutros M. Wnt signaling in cancer. Oncogene 2017; 36(11): 1461–1473
29. Gruszka AM, Valli D, Alcalay M. Wnt signalling in acute myeloid leukaemia. Cells 2019; 8(11): 1403
30. Wang Y, Krivtsov AV, Sinha AU, North TE, Goessling W, Feng Z, Zon LI, Armstrong SA. The Wnt/beta-catenin pathway is required for the development of leukemia stem cells in AML. Science 2010; 327(5973): 1650–1653
31. Willert K, Brown JD, Danenberg E, Duncan AW, Weissman IL, Reya T, Yates JR 3rd, Nusse R. Wnt proteins are lipid-modified and can act as stem cell growth factors. Nature 2003; 423(6938): 448–452
32. Gao X, Hannoush RN. Single-cell imaging of Wnt palmitoylation by the acyltransferase porcupine. Nat Chem Biol 2014; 10(1): 61–68
33. Nile AH, Hannoush RN. Fatty acylation of Wnt proteins. Nat Chem Biol 2016; 12(2): 60–69
34. Miranda M, Galli LM, Enriquez M, Szabo LA, Gao X, Hannoush RN, Burrus LW. Identification of the WNT1 residues required for palmitoylation by Porcupine. FEBS Lett 2014; 588(24): 4815–4824
35. Gharib E, Nasrinasrabadi P, Zali MR. Development and validation of a lipogenic genes panel for diagnosis and recurrence of colorectal cancer. PLoS One 2020; 15(3): e0229864
36. Gharib E, Nasri Nasrabadi P, Reza Zali M. miR-497-5p mediates starvation-induced death in colon cancer cells by targeting acyl-CoA synthetase-5 and modulation of lipid metabolism. J Cell Physiol 2020; 235(7–8): 5570–5589
37. Zhang L, Lv J, Chen C, Wang X. Roles of acyl-CoA synthetase long-chain family member 5 and colony stimulating factor 2 in inhibition of palmitic or stearic acids in lung cancer cell

proliferation and metabolism. Cell Biol Toxicol 2021; 37(1): 15–34

38. Tomoda H, Igarashi K, Cyong JC, Omura S. Evidence for an essential role of long chain acyl-CoA synthetase in animal cell proliferation. Inhibition of long chain acyl-CoA synthetase by triacsins caused inhibition of Raji cell proliferation. J Biol Chem 1991; 266(7): 4214–4219
39. Mashima T, Sato S, Okabe S, Miyata S, Matsuura M, Sugimoto Y, Tsuruo T, Seimiya H. Acyl-CoA synthetase as a cancer survival factor: its inhibition enhances the efficacy of etoposide. Cancer Sci 2009; 100(8): 1556–1562
40. Liu F, Kalpage HA, Wang D, Edwards H, Hüttemann M, Ma J, Su Y, Carter J, Li X, Polin L, Kushner J, Dzinic SH, White K, Wang G, Taub JW, Ge Y. Cotargeting of mitochondrial complex I and Bcl-2 shows antileukemic activity against acute myeloid leukemia cells reliant on oxidative phosphorylation. Cancers (Basel) 2020; 12(9): 2400
41. Valentin R, Grabow S, Davids MS. The rise of apoptosis: targeting apoptosis in hematologic malignancies. Blood 2018; 132(12): 1248–1264